THE JOURNAL OF BIOLOGICAL CHEMISTRY VOL. 288, NO. 9, pp. 6522–6533, March 1, 2013

Hydralazine and Organic Nitrates Restore Impaired Excitation-Contraction Coupling by Reducing Calcium Leak Associated with Nitroso-Redox Imbalance*[S]

Received for publication, August 21, 2012, and in revised form, December 17, 2012 Published, JBC Papers in Press, January 14, 2013, DOI 10.1074/jbc.M112.412130

Raul A. Dulce[‡1], Omer Yiginer[§¶1], Daniel R. Gonzalez[‖], Garrett Goss[‡], Ning Feng[¶], Meizi Zheng[**], and Joshua M. Hare[‡2]

*From the [‡]Interdisciplinary Stem Cell Institute (ISCI), University of Miami Miller School of Medicine, Miami, Florida 33136, the [§]Department of Cardiology, Gulhane Military Medical Academy, Haydarpasa Hospital, 34668 Istanbul, Turkey, the [¶]Division of Cardiology, Johns Hopkins School of Medicine, Baltimore, Maryland 21287, the [‖]Departamento de Ciencias Basicas Biomedicas, Facultad de Ciencias de la Salud, Universidad de Talca, 3460000 Talca, Chile, and the **Center for Integrative Medicine, School of Medicine, University of Maryland, Baltimore, Maryland 21207*

Background: Hydralazine and organic nitrates have clinical benefits for heart failure, but the underlying mechanism is controversial.
Results: Hydralazine reduced sarcoplasmic reticulum Ca^{2+} leak and improved Ca^{2+} cycling and contractility; nitroglycerin enhanced contractile efficiency; both were impaired by nitroso-redox imbalance.
Conclusion: These agents exert complementary effects on nitroso-redox imbalance.
Significance: New mechanistic insights for redox-targeted treatments of heart failure.

Although the combined use of hydralazine and isosorbide dinitrate confers important clinical benefits in patients with heart failure, the underlying mechanism of action is still controversial. We used two models of nitroso-redox imbalance, neuronal NO synthase-deficient ($NOS1^{-/-}$) mice and spontaneously hypertensive heart failure rats, to test the hypothesis that hydralazine (HYD) alone or in combination with nitroglycerin (NTG) or isosorbide dinitrate restores Ca^{2+} cycling and contractile performance and controls superoxide production in isolated cardiomyocytes. The response to increased pacing frequency was depressed in $NOS1^{-/-}$ compared with wild type myocytes. Both sarcomere length shortening and intracellular Ca^{2+} transient ($\Delta[Ca^{2+}]_i$) responses in $NOS1^{-/-}$ cardiomyocytes were augmented by HYD in a dose-dependent manner. NTG alone did not affect myocyte shortening but reduced $\Delta[Ca^{2+}]_i$ across the range of pacing frequencies and increased myofilament Ca^{2+} sensitivity thereby enhancing contractile efficiency. Similar results were seen in failing myocytes from the heart failure rat model. HYD alone or in combination with NTG reduced sarcoplasmic reticulum (SR) leak, improved SR Ca^{2+} reuptake, and restored SR Ca^{2+} content. HYD and NTG at low concentrations (1 μM), scavenged superoxide in isolated cardiomyocytes, whereas in cardiac homogenates, NTG inhibited xanthine oxidoreductase activity and scavenged NADPH oxidase-dependent superoxide more efficiently than HYD. Together, these results revealed that by reducing SR Ca^{2+} leak, HYD improves Ca^{2+} cycling and contractility impaired by nitroso-redox imbalance, and NTG enhanced contractile efficiency, restoring cardiac excitation-contraction coupling.

Heart failure (HF)[3] is a common and increasingly prevalent cause of morbidity and mortality. Prior to the African-American heart failure trial, the only pharmacologic strategy that improved survival in HF was neurohormonal blockade therapy. This trial revealed increased survival among African-American patients with advanced HF treated with the combination of isosorbide dinitrate (ISDN) and hydralazine (HYD) (1–3). However, the precise mechanism(s) by which this regimen reduced mortality remains unclear.

HF is characterized by impaired excitation-contraction (E-C) coupling. For instance, increased contractile force upon increasing frequency of stimulation (force-frequency relationship, FFR) is compromised in failing hearts, giving rise to a blunted or negative FFR (4–6). Defects in calcium (Ca^{2+}) handling may be responsible for this phenomenon (7, 8). It is increasingly appreciated that altered signaling in both Ca^{2+} reuptake mechanisms and Ca^{2+} leak through the ryanodine receptor (RyR2) contribute to impairment of the Ca^{2+} cycle in the failing heart. In this regard, Ca^{2+} leak is believed to be mediated by post-translational modifications of the RyR2, associated with nitroso-redox (NO/redox) imbalance (9, 10), a linked abnormality in the failing myocardium (11, 12). As a

* This work was supported, in whole or in part, by National Institutes of Health Grants HL-65455, 5R01AG025017, and R01 HL094849 (to J. M. H.).
[S] This article contains supplemental Tables S1–S3.
[1] Both authors contributed equally to this work.
[2] To whom correspondence should be addressed: Biomedical Research Building (BRB), 1501 NW 10th Ave., Room 916, Miami, FL 33136. Tel.: 305-243-5579; Fax: 305-243-5584; E-mail: JHare@med.miami.edu.

[3] The abbreviations used are: HF, heart failure; CM, cardiomyocyte; E-C, excitation-contraction; FFR, force-frequency response; HYD, hydralazine; ISDN, isosorbide dinitrate; NTG, nitroglycerin; NO/redox, nitroso-redox; $NOS1^{-/-}$, neuronal nitric-oxide synthase deficient mice; NOX, NADPH oxidase; $ONOO^-$, peroxynitrite; PLB, phospholamban; ROS, reactive oxygen species; RyR2, cardiac ryanodine receptor; SERCA2, SR Ca^{2+}-ATPase 2; SHHF, spontaneously hypertensive heart failure rats; SL, sarcomere length; SR, sarcoplasmic reticulum; WKY, Wistar Kyoto; XOR, xanthine oxidoreductase; DHE, dihydroethidium; ANOVA, analysis of variance.

consequence of the sarcoplasmic reticulum (SR) Ca^{2+} leak, an altered E-C coupling occurs by depleting the SR Ca^{2+} stores resulting in possible impaired contractile function of the heart.

Increased xanthine oxidoreductase (XOR)-, and possibly NADPH oxidase (NOX)-mediated reactive oxygen species (ROS) production also occurs in failing hearts (13–15). Importantly, disruption in signaling pathways due to oxidative stress can be intensified by NO deficiency, a situation of NO/redox disequilibrium (16, 17). One possible explanation of the clinical benefits of HYD-ISDN is restoration of the balance between formation of reactive oxygen and reactive nitrogen species (2).

We used two established models of cardiac NO/redox imbalance to test the hypothesis that HYD and organic nitrates restore NO bioavailability and reactivity, ameliorate NO/redox disequilibrium, and improves myocardial contractility as measured by FFR. Accordingly, we examined the effects of each drug, alone and in combination, on sarcomere length (SL) shortening, Ca^{2+} cycling, and SR Ca^{2+} leak in neuronal NO synthase-deficient ($NOS1^{-/-}$) mice and spontaneously hypertensive heart failure (SHHF) rats. ROS production by XOR and NOX were determined *in vitro* in $NOS1^{-/-}$ hearts.

EXPERIMENTAL PROCEDURES

Animal Models and Myocyte Isolation—All protocols and experimental procedures were approved by the Institutional Animal Care and Use Committee of The University of Miami following the Guide for the Care and Use of Laboratory Animals (NIH Publication 85–234, revised 1996).

Cardiomyocytes (CMs) were isolated from C57BL/6J mice (WT, 3–5 months old, $n = 25$; Jackson Laboratories, Bar Harbor, ME) and transgenic mice with homozygous deletions for NOS1 (B6;129S4-Nos1<tm1Plh>J, 3–5 months old, $n = 41$) or male SHHF rats (22–24 months old, $n = 4$; Charles River Laboratories Inc., Wilmington, MA) and their normotensive controls, Wistar Kyoto rats (WKY, $n = 5$) hearts as described in detail (18). Briefly, hearts were harvested and retrograde perfused through the aorta in a modified Langendorf system with an isolation solution containing collagenase type 2 (Worthington Biochemical Corp.) and protease type XIV (Sigma).

Protocols—Cells were loaded with Fura-2. The SL and intracellular Ca^{2+} concentration ($[Ca^{2+}]_i$) were measured simultaneously in CMs stimulated at 0.5, 1, 2, 3, and 4 Hz. Experiments were repeated after a 10-min incubation with HYD (0.1, 1, and 10 μM; Sigma), nitroglycerin (NTG, 0.1, 1 and 10 μM; American Regent Laboratories, Inc., Shirley, NY), 10 μM ISDN (Alexis Biochemicals, Enzo Life Sciences, Inc., PA), or HYD plus either NTG or ISDN. Experiments in SHHF rat CMs were carried out similarly, with the exception that the concentration of drugs was as follows: 10 μM HYD, 10 μM NTG, and their combination. All experiments were conducted at 37 °C.

Contractility and Ca^{2+} Measuring—SL shortening (%ΔSL) was recorded with an IonOptix iCCD camera and calculated as: (resting SL − peak SL) × 100/resting SL. $Ca^{2+}{}_i$ was measured using a dual excitation (340/380 nm) spectrofluorometer (IonOptix LLC, Milton, MA). The "*in vivo*" calibration was performed using solutions containing 10 μM ionomycin (Sigma) as described by Grynkiewicz *et al.* (19) and the $[Ca^{2+}]_i$ was calculated using the following equation,

$$[Ca^{2+}]_i = K'_d \times (Sf_2/Sb_2) \times (R - R_{min})/(R_{max} - R) \quad \text{(Eq. 1)}$$

where K_d' (apparent dissociation constant for Fura-2) in adult myocytes was 224 nM. R_{min} and R_{max} as well as the scaling factors (Sf_2 and Sb_2) were extracted from the calibration curves. $\Delta[Ca^{+2}]_i$ amplitude was considered as: peak $[Ca^{+2}]_i$ − resting $[Ca^{+2}]_i$.

SR Ca^{2+} Leak and SR Ca^{2+} Load Measurement—SR Ca^{2+} leakage was assessed with tetracaine as described by Shannon *et al.* (20). Briefly, after pacing was stopped, a fast switch to a 0 Na^+, 0 Ca^{2+} Tyrode solution (Na^+ was replaced by an equimolar amount of Li^+) was performed. After 60 s, similar to Bassani *et al.* (21), a rapid switching to 0 Na^+, 0 Ca^{2+} solution containing 20 mM caffeine to assess SR Ca^{2+} content was applied. Following recovery of the cell, the same pacing protocol was assessed. After stop pacing, a switch to 0 Na^+, 0 Ca^{2+} Tyrode solution containing 1 mmol/liter of tetracaine (Sigma) was performed. The observed drop in the Fura-2 ratio compared with the nontetracaine treated condition was considered the Ca^{2+} leak for a particular CM. After assessing the Ca^{2+} leak, tetracaine was washed out by superfusing fresh 0 Na^+, 0 Ca^{2+} Tyrode solution and then a new caffeine challenge was applied to estimate the SR Ca^{2+} load. SR Ca^{2+} contents were calculated considering that SR represents 3.5% and cytosol 65% of the CM volumes. The following equation from Shannon *et al.* (20) was used: $[Ca^{2+}]_{SR} = [Ca^{2+}]_{caff} + (\beta_{max\text{-}SR} \times [Ca^{2+}]_{caff})/([Ca^{2+}]_{caff} + K_{d\text{-}SR})$. $[Ca^{2+}]_{SR}$ is the SR Ca^{2+} content, $[Ca^{2+}]_{caff}$ is the SR Ca^{2+} released by caffeine, $\beta_{max\text{-}SR}$ and $K_{d\text{-}SR}$ are the usual Michaelis parameters for SR Ca^{2+} binding. SR leak-SR load pairs were grouped by comparable SR Ca^{2+} loads and expressed as a leak-load relationship.

Detection of Superoxide by DHE Staining—Fresh isolated mouse CMs were incubated at room temperature for 30 min with dihydroethidium (DHE, 3 μM; Molecular Probes). After washing with PBS, cells were fixed with 2% paraformaldehyde for 5 min at 4 °C. Finally, the samples were mounted in Prolong Gold anti-fade (Invitrogen). The images were obtained using a Zeiss LSM-710 confocal microscope. Nuclear fluorescence captured at 562 nm was quantified using the Image-Pro plus software (MediaCybernetics, Silver Spring, MD) and normalized by cytosolic fluorescence.

NOX-dependent Superoxide Production—NOX-dependent superoxide production was measured in heart homogenates from $NOS1^{-/-}$ mice using lucigenin (5 μM)-enhanced chemiluminescence (β-NADPH 300 μM; room temperature) on a microplate luminometer (Veritas, Turner Biosystems, Sunnyvale, CA). Chemiluminescence readings were expressed as integrated light units. Experiments were performed in the presence of increasing concentrations of HYD and NTG (0.01, 0.1, and 1 mM).

XOR Activity—XOR activity was investigated by measuring uric acid (22) and superoxide production. Heart homogenates from $NOS1^{-/-}$ mice were passed through a Sephadex G-25 column (GE Healthcare) and XOR-dependent superoxide production was measured using Amplex Red (Molecular Probes,

Eugene, OR). The effluent was assessed at 295 nm for uric acid. Both assay plates were incubated at 37 °C for 30 min in the presence or absence of allopurinol, and HYD and NTG at increasing concentrations.

Assessment of Ca^{2+} Myofilament Responsiveness—Myofilament responsiveness to Ca^{2+} was assessed using the steady-state relationship between SL and $[Ca^{2+}]_i$ in intact single CMs tetanized by high-frequency (10 Hz) stimulation after exposure to thapsigargin (0.2 μM for 15 min), as described previously (23). With this approach, the $Ca^{2+}{}_i$ was reversibly clamped during the tetanic contracture for 20 s and then rapidly returned to resting levels upon cessation of electrical stimulation via the Na^+/Ca^{2+} exchanger. The steady-state levels of Ca^{2+} achieved during tetanus exposure were regulated by subjecting CMs to Tyrode solutions containing increasing concentrations of Ca^{2+} (0.1, 1.0, 5.0, 10, and 20 mM $CaCl_2$).

Western Blot Immunoanalysis—Hearts from 12 $NOS1^{-/-}$ mice were perfused with Krebs solution (30 min; $n = 6$), or Krebs plus 10 μM HYD (30 min; $n = 4$), or 10 μM ISDN (30 min; $n = 2$). Hearts were homogenized in cold RIPA buffer containing the protease inhibitor mixture and phosphatase inhibitors. Samples were electrophoresed using a NuPAGE 10% Bis-Tris gel (Invitrogen) and transferred to PVDF membranes (Bio-Rad Laboratories). Immunoblot analysis was performed with goat polyclonal antibody for SERCA2 (Santa Cruz Biotechnology, Inc.), mouse monoclonal antibody for phospholamban (PLB; Pierce, Thermo Scientific), rabbit polyclonal for phospho-PLB-(Ser16) (Pierce, Thermo Scientific), PLB phospho Thr-17 (Badrilla, Leeds, UK), NCX1 (RDI, Flanders, NJ), and GAPDH (as loading control; Santa Cruz). Phosphorylated PLB were expressed as a ratio of Ser(P)-16/PLB or Thr(P)-17/PLB and SERCA2, NCX1, or total PLB expression compared with GAPDH.

Statistical Analysis—Data are reported as mean ± S.E. Statistical significance was determined by unpaired Student's *t* test, one-way ANOVA, or two-way ANOVA followed by Student's-Newman-Keuls or Bonferonni's post hoc tests, as appropriate, using the GraphPad Prism version 4.02 (GraphPad Prism Software Corporation, San Diego, CA). The null hypothesis was rejected at $p < 0.05$.

RESULTS

Hydralazine and Organic Nitrates Improved Contractility in $NOS1^{-/-}$ CMs—To determine the effect of the drugs on CM contractility, we measured SL shortening in cells from WT and $NOS1^{-/-}$ mice paced at 0.5, 1, 2, 3, and 4 Hz (Fig. 1, *A* and *B*). At baseline, SL shortening was similar in $NOS1^{-/-}$ and WT CMs (0.5 Hz; Table 1). However, as previously described (12), the increased SL shortening due to augmented pacing frequency was blunted in $NOS1^{-/-}$ CMs compared with WT (4Hz, Table 1, and Fig. 1, *A* and *B*, $p < 0.0001$ *versus* WT, two-way ANOVA).

HYD augmented the frequency-dependent SL shortening in $NOS1^{-/-}$ CMs in a concentration-dependent manner (Figs. 1*C* and 2*E*, supplemental Table S1). In contrast, NTG alone did not affect the SL shortening in $NOS1^{-/-}$ (Fig. 1*C*, supplemental Table S1). To test whether the drug combination would have a synergistic effect, $NOS1^{-/-}$ myocytes were incubated with

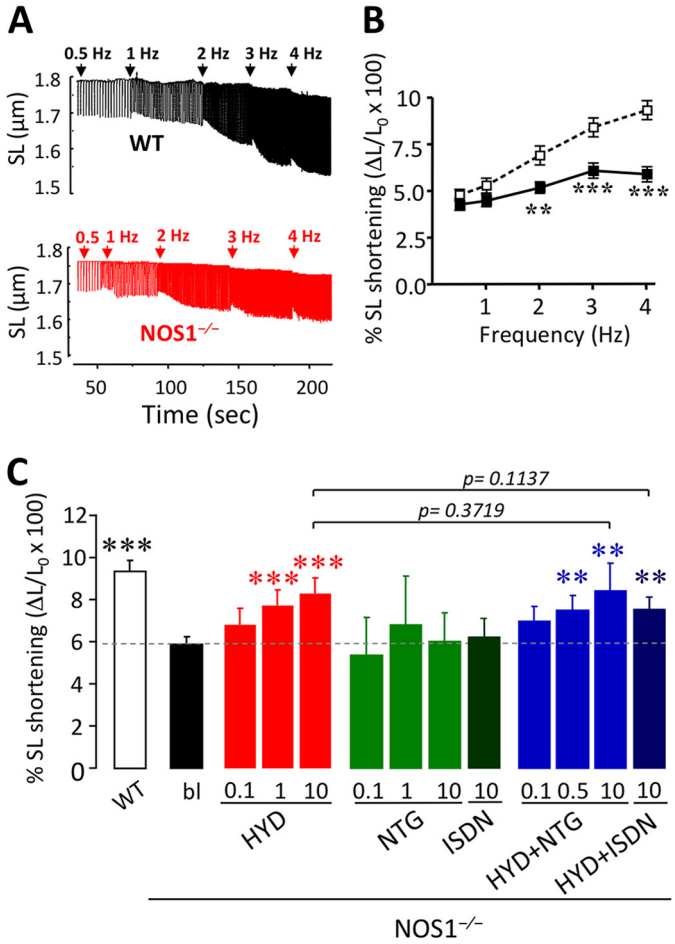

FIGURE 1. **Contractile performance in $NOS1^{-/-}$ cardiomyocytes.** *A*, representative traces of SL in WT (*black*) and $NOS1^{-/-}$ (*red*) CMs under increasing rates of pacing from 0.5 to 4 Hz. *B*, CM contractility expressed as % SL shortening *versus* resting SL, in $NOS1^{-/-}$ (■; $n = 50–54$ cells) compared with WT (□; $n = 34–41$ cells). *C*, SL shortening at 4 Hz expressed as the percentage of shortening *versus* resting SL, in WT control or $NOS1^{-/-}$ CMs in the absence (*bl*) or presence of HYD (0.1, 1 or 10 μM), NTG (0.1, 1, or 10 μM), ISDN (10 μM), and a combination (HYD + NTG, 0.1, 0.5 or 10 μM each and HYD + ISDN; 10 μM each). **, $p < 0.01$; ***, $p < 0.001$ *versus* WT control, two-way ANOVA.

HYD plus NTG. Although this treatment restored the FFR in a dose-dependent manner, the response was not greater than hydralazine alone (Figs. 1*C* and 2*E*, Supplemental Table 1). In WT CMs, neither HYD nor NTG, alone or in combination, affected frequency-dependent SL shortening (data not shown).

We next assessed whether ISDN, the pharmacologically employed nitrate, had similar effects as NTG. Indeed, the combination of HYD and ISDN also induced an increased frequency-dependent SL shortening in $NOS1^{-/-}$ compared with untreated $NOS1^{-/-}$ CMs (Fig. 1*C* and supplemental Table S1; $p = 0.004$) at an equimolar concentration of 10 μM. Similar to NTG, 10 μM ISDN did not alter contractility in $NOS1^{-/-}$ (Fig. 1*C* and supplemental Table S1).

Divergent Effects of Hydralazine and Nitroglycerin on Ca^{2+} Transient in $NOS1^{-/-}$ CMs—Resting diastolic $[Ca^{2+}]_i$ values were slightly elevated in $NOS1^{-/-}$ compared with WT CMs, over the range of studied frequencies (Table 1; $p < 0.01$) as previously described (12, 24). When the $[Ca^{2+}]_i$ transient ($\Delta[Ca^{2+}]_i$) was studied, $[Ca^{2+}]_i$-FFR was clearly depressed in $NOS1^{-/-}$ CMs compared with WT, as previously described

TABLE 1
Baseline myocyte performance

	WT		$NOS1^{-/-}$	
	0.5 Hz	4 Hz	0.5 Hz	4 Hz
Cells[a]	40–41	32–34	50–54	40–50
SL shortening (%)[b]	4.75 ± 0.30	9.30 ± 0.50	4.27 ± 0.30	5.90 ± 0.40[c]
Diastolic $[Ca^{2+}]_i$ (nM)	234 ± 16	298 ± 26	284 ± 19[d]	337 ± 19
$\Delta[Ca^{2+}]_i$ transient (nM)	160 ± 13	315 ± 40	254 ± 19[e]	278 ± 21
$\Delta[Ca^{2+}]_i$ decay (τ s)	0.198 ± 0.009	0.091 ± 0.004	0.231 ± 0.013[d]	0.101 ± 0.006
SR Ca^{2+} load (μM)	42.0 ± 7.4	70.6 ± 7.5	37.9 ± 7.2	52.4 ± 4.7[d]

[a] Five to 10 cells per heart were studied.
[b] SL shortening is calculated as: (resting SL − peak SL)/resting SL × 100.
[c] $p < 0.001$ *versus* WT (unpaired Student's *t* test).
[d] $p < 0.05$ *versus* WT (unpaired Student's *t* test).
[e] $p < 0.01$ *versus* WT (unpaired Student's *t* test).

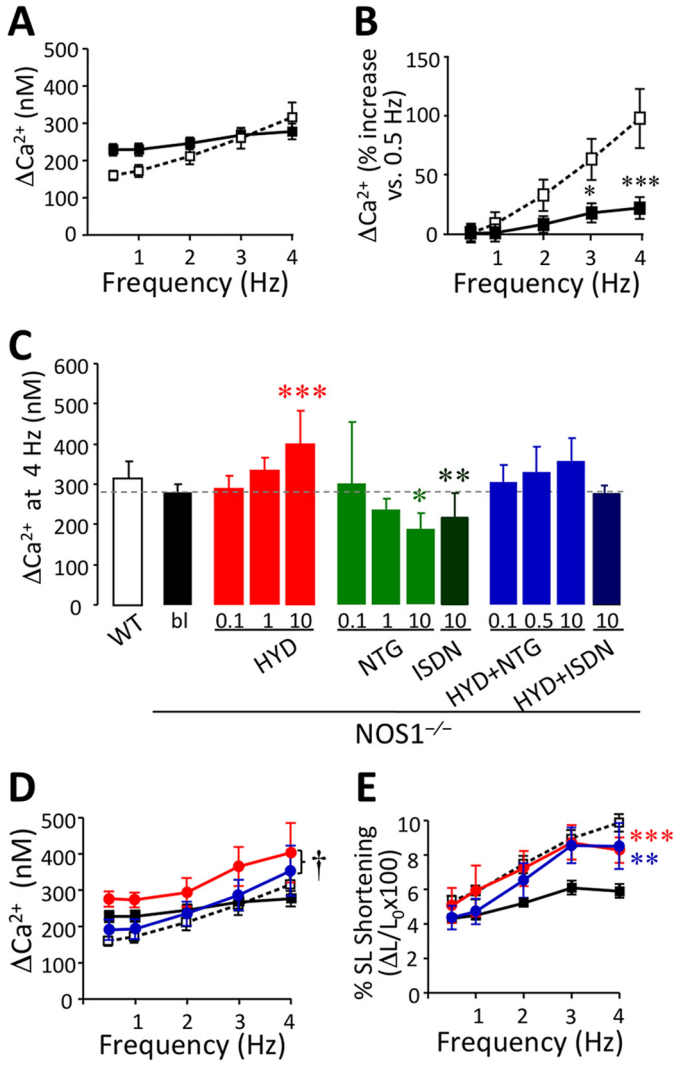

FIGURE 2. **Intracellular Ca^{2+} transient ($\Delta[Ca^{2+}]_i$) in $NOS1^{-/-}$ cardiomyocytes.** *A*, $\Delta[Ca^{2+}]_i$ (nM) in $NOS1^{-/-}$ (■; $n = 40–50$ cells) compared with WT (□; $n = 32–40$ cells). *B*, $\Delta[Ca^{2+}]_i$ in $NOS1^{-/-}$ (■) and WT (□) CMs, expressed as % increase *versus* 0.5 Hz. *C*, $\Delta[Ca^{2+}]_i$ at 4 Hz in WT control or $NOS1^{-/-}$ CMs in the absence (*bl*) or presence of HYD (0.1, 1 or 10 μM), NTG (0.1, 1 and 10 μM), ISDN (10 μM), and a combination (HYD + NTG; 0.1, 0.5, and 10 μM each; and HYD + ISDN; 10 μM each). *D*, ΔCa^{2+} frequency response in WT CMs (□) under baseline conditions or $NOS1^{-/-}$ baseline (■) or treated with 10 μM HYD (*red circle*) or 10 μM HYD + NTG (*blue circle*). *E*, FFR in CMs under the same conditions as mentioned above. The combination induces a significant increase in FFR but does not change ΔCa^{2+} significantly compared with $NOS1^{-/-}$ CMs. However, the contractile reserve is restored. *, $p < 0.05$; **, $p < 0.01$; and ***, $p < 0.001$ *versus* $NOS1^{-/-}$ control; †, $p < 0.05$ *versus* HYD alone; two-way ANOVA.

(Fig. 2, *A* and *B*, $p < 0.0001$ *versus* WT; two-way ANOVA) (18, 24, 25). HYD induced a $\Delta[Ca^{2+}]_i$ increase in a concentration-dependent manner (Fig. 2*C*) as well as significantly increased the $[Ca^{2+}]_i$-FFR (Fig. 2*D*, supplemental Table S2, $p < 0.05$). Thus, the increase in contractility in response to HYD was mirrored by a concomitant increase in $\Delta[Ca^{2+}]_i$ (Fig. 2*E*).

Although NTG did not affect contractility, it induced a concentration-dependent decrease in the $\Delta[Ca^{2+}]_i$ amplitude compared with control $NOS1^{-/-}$ myocytes most clearly seen at 4 Hz. This decrease was reproduced using 10 μM ISDN (Fig. 2*C* and supplemental Table S2). The combination of HYD and NTG (Fig. 2*D*) or ISDN (supplemental Table S2) on $NOS1^{-/-}$ CMs restored the increasing $[Ca^{2+}]_i$-FFR (frequency $p = 0.0213$ or $p = 0.0014$, respectively; two-way ANOVA) by reducing the $\Delta[Ca^{2+}]_i$ amplitude toward the levels in WT CMs ($p = 0.042$ or $p = 0.0005$ *versus* HYD alone, respectively). Thus, for any given improvement in cardiac contraction due to HYD, organic nitrates offset the increase in $[Ca^{2+}]_i$, thereby enhancing contractile efficiency (Fig. 2, *D* and *E*). Neither HYD nor NTG, alone or in combination (10 μM), altered the $[Ca^{2+}]_i$-FFR in WT CMs (data not shown).

We also examined the peak $[Ca^{2+}]_i$ decay time constant (τ), which was significantly higher in $NOS1^{-/-}$ than WT CMs ($p < 0.0001$, Table 1, Fig. 3, *A* and *B*). All treatments accelerated τ (particularly at 0.5 Hz, Fig. 3*B* and supplemental Table S3) in a dose-dependent manner ($p < 0.0001$ HYD alone or in combination with NTG *versus* $NOS1^{-/-}$ baseline; $p = 0.001$ NTG alone *versus* $NOS1^{-/-}$ baseline, two-way ANOVA). ISDN was equally effective in reducing τ, either alone or combined with 10 μM HYD ($p < 0.001$; supplemental Table S3). Reuptake of Ca^{2+} assessed by decay of caffeine-induced Ca^{2+} transients in a Na^+ and Ca^{2+}-free solution, which avoids any Ca^{2+} flux throughout the sarcolemma, was slower in $NOS1^{-/-}$ ($K = 0.1888$/s; $T_{50} = 3.65 \pm 0.12$ s, fitted by an one-phase exponential equation) compared with WT cells ($K = 0.2724$/s; $T_{50} = 2.53 \pm 0.08$ s; $p = 0.0005$). Treatment with either 10 μM HYD or NTG increased the SR Ca^{2+} reuptake rate in $NOS1^{-/-}$ ($K = 0.240$/s, $T_{50} = 2.88 \pm 0.17$ s, $p = 0.0003$ and $K = 0.2392$/s, $T_{50} = 2.88 \pm 0.11$ s, $p < 0.0001$, respectively). The combination exerted an additive effect ($K = 0.2919$/s, $T_{50} = 2.36 \pm 0.06$ s, $p < 0.0001$) suggesting that the improvement in the regular field-stimulated $\Delta[Ca^{2+}]_i$ decay was mediated by enhanced SERCA2 activity. This speculation was confirmed by assessing phosphorylation of PLB in cardiac homogenates from $NOS1^{-/-}$ hearts treated with either

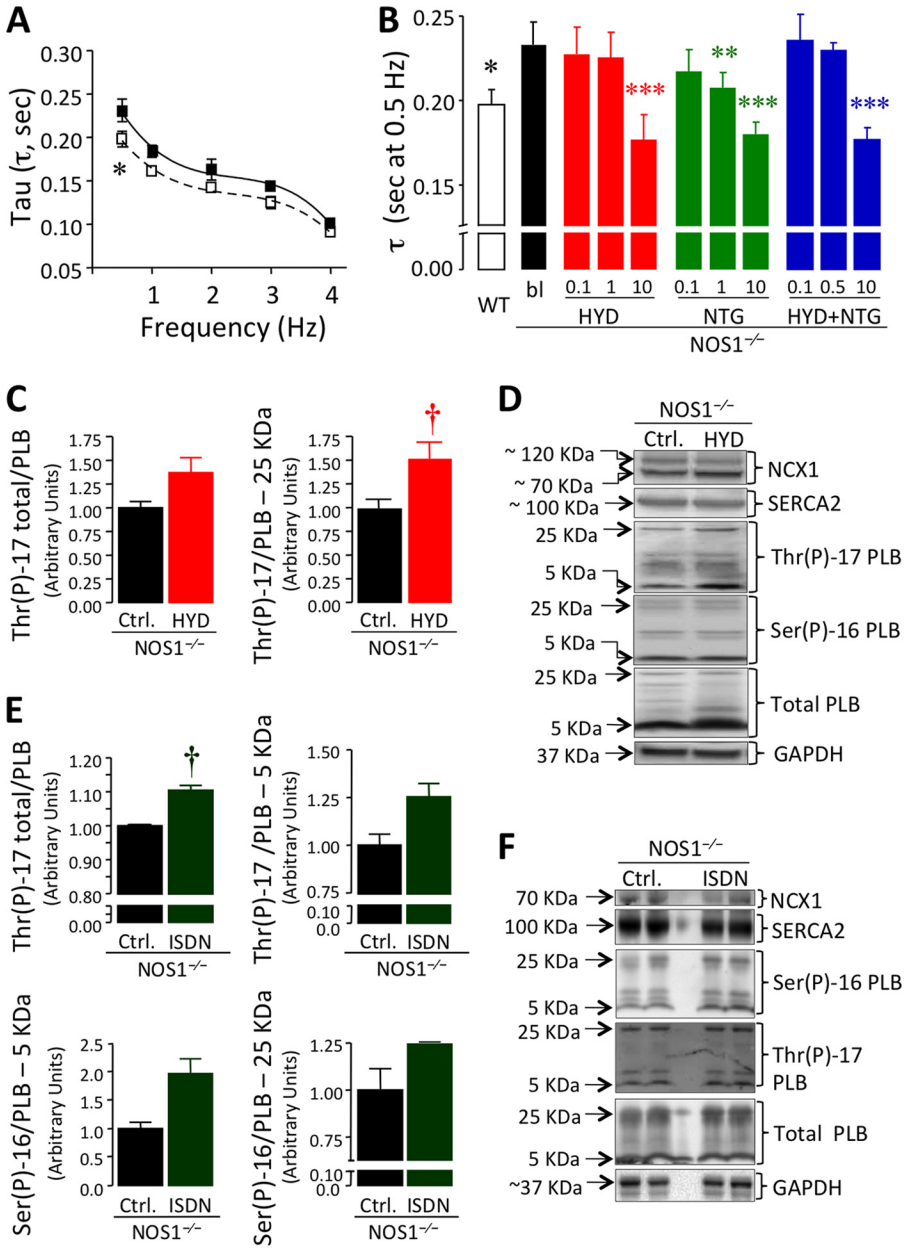

FIGURE 3. **Hydralazine and organic nitrates enhance Ca^{2+} influx to the SR in $NOS1^{-/-}$ cardiomyocytes.** *A*, Ca^{2+} decay time constant (tau, τ) *versus* frequency in $NOS1^{-/-}$ (■) compared with WT (□) CMs. *B*, Tau values at 0.5 Hz in WT control or $NOS1^{-/-}$ CMs treated with or without HYD, NTG, or a combination (HYD + NTG) at the indicated concentrations (μM) (n = 5–21 cells) (*, $p < 0.05$; **, $p < 0.01$; and ***, $p < 0.001$ *versus* $NOS1^{-/-}$ control; two-way ANOVA). *C*, PLB phosphorylation at threonine 17 (Thr(P)-17) in baseline or 10 μM HYD-treated $NOS1^{-/-}$ hearts (total and pentameric Thr(P)-17 PLB). *D*, representative Western blots for all studied proteins in the absence or presence of 10 μM HYD. *E*, PLB Thr(P)-17 in baseline or 10 μM ISDN-treated $NOS1^{-/-}$ hearts (total and monomeric Thr(P)-17 PLB). Phosphorylated PLB at Ser-16 (Ser(P)-16, *bottom*) was also measured. *F*, representative Western blots. No significant changes were observed in Ser(P)-16, SERCA2, or NCX1 with either treatment. †, $p < 0.05$ *versus* $NOS1^{-/-}$ control; Student's *t* test.

10 μM HYD or ISDN. HYD increased phosphothreonine 17 (Thr(P)-17) for pentameric PLB ($p = 0.0393$); but not on total PLB ($p = 0.0597$) or monomeric PLB (Fig. 3, *C* and *D*). ISDN increased total Thr(P)-17 ($p = 0.011$; Fig. 3, *E* and *F*). Neither treatment significantly increased phosphoserine 16 (Ser(P)-16; Fig. 3, *D–F*).

Hydralazine Alone and in Combination with Nitroglycerin, Lowers SR Ca^{2+} Leakage Toward Normal—We next assessed SR Ca^{2+} leak and the SR Ca^{2+} leak-load relationship, using the technique of Shannon *et al.* (20) using tetracaine, a RyR2 blocker (Fig. 4*A*). SR Ca^{2+} leak was augmented in $NOS1^{-/-}$ ($R^2 = 0.5225$ for WT and $R^2 = 0.8827$ for $NOS1^{-/-}$, Fig. 4*B*; $p =$ 0.0002). The decreased SR Ca^{2+} content and increased diastolic Ca^{2+} exhibited by $NOS1^{-/-}$ compared with WT CMs are consistent with the elevated Ca^{2+} leak. HYD reduced the leak in a concentration-dependent manner in $NOS1^{-/-}$ myocytes (Fig. 4*C*; $p = 0.0012$). Neither 1 nor 10 μM HYD significantly affected the SR Ca^{2+} leak in WT CMs (data not shown).

NTG did not significantly affect the SR Ca^{2+} leak in $NOS1^{-/-}$ cells (Fig. 4*D*). In contrast, the combination of NTG plus HYD reduced the leak in a concentration-dependent manner as shown by the leak-load relationship (Fig. 4*E*; $p = 0.0001$). Fig. 4*F* shows the drug concentration-SR Ca^{2+} leak response relationship. The IC_{50} for HYD was 0.0705 ± 0.0473 μM (at

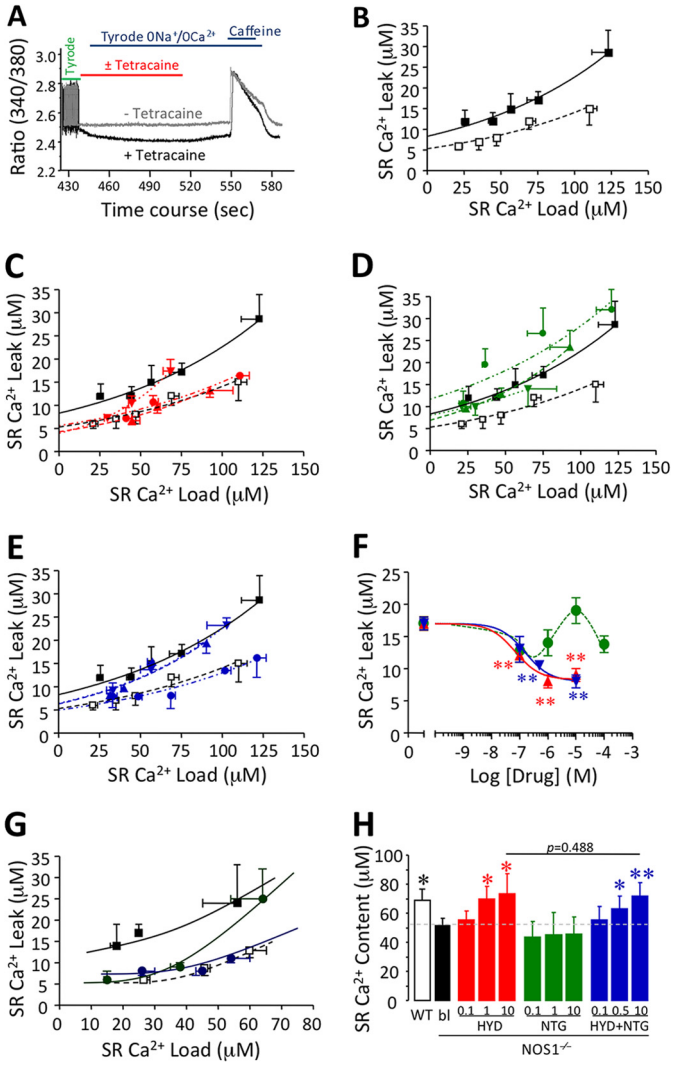

FIGURE 4. **Assessment of SR diastolic Ca^{2+} leakage in the presence of hydralazine, organic nitrates, or their combination.** *A*, protocol to assess the SR Ca^{2+} leak using tetracaine to block RyR2 and caffeine to estimate the SR Ca^{2+} content. *B*, SR Ca^{2+} load-leak relationship in WT (□) and NOS1$^{-/-}$ (■) CMs. *C*, SR Ca^{2+} load-leak relationship in NOS1$^{-/-}$ CMs in the absence (red ■) or presence of HYD (0.1 μM, *red* ▼, 1 μM *red* ▲ or 10 μM, *red* ●). *D*, in the presence of NTG (0.1 μM, *green* ▼; 1 μM, *green* ▲; or 10 μM, *green* ●). *E*, in the presence HYD plus NTG (0.1 μM, *blue* ▼; 0.5 μM, *blue* ▲; or 10 μM, *blue* ●). NOS1$^{-/-}$ CMs exhibited an increased SR Ca^{2+} leak and HYD alone or a combination reduced it in a dose-dependent manner. *F*, dose-response relationship; effect of increasing concentrations of HYD (*red* ▲), NTG (*green* ●), and a combination of HYD + NTG (*blue* ▼) on SR Ca^{2+} leak in NOS1$^{-/-}$ CMs (**, $p <$ 0.01 *versus* nontreated NOS1$^{-/-}$ CMs; one-way ANOVA). *G*, SR Ca^{2+} load-leak curves in NOS1$^{-/-}$ (■) CMs in the absence or presence of 10 μM ISDN alone (*dark green* ●) or in combination with 10 μM HYD (*dark blue* ●). Load-leak relationship of WT was included as normal control (□). *H*, SR Ca^{2+} content at 4 Hz. HYD alone and in combination with NTG restored the SR Ca^{2+} content in NOS1$^{-/-}$ in a concentration-dependent manner toward normal levels as exhibited by WT CMs. NTG alone had no significant effects. *, $p < 0.05$ and **, $p < 0.01$ *versus* NOS1$^{-/-}$ control; two-way ANOVA.

matched SR load of 50 μM). The combination exerted a comparable effect to HYD alone (IC_{50} = 0.160 ± 0.128 μM).

The combination of 10 μM HYD and 10 μM ISDN reduced the SR Ca^{2+} leak in NOS1$^{-/-}$ equal to HYD plus NTG (Fig. 4*G*; $p = 0.0186$). ISDN alone exhibited differential effects at the low SR Ca^{2+} load (reduced leak) compared with the higher load (no effect) in NOS1$^{-/-}$ CMs (Fig. 4*G*). We also assessed the effects of 10 μM HYD plus 10 μM NTG on the SR Ca^{2+} leak in WT CMs but found no significant difference compared with control, whereas 10 μM NTG significantly reduced the degree of the SR Ca^{2+} leak in WT (data not shown).

Cardiomyocyte SR Ca^{2+} Content—Because SR Ca^{2+} storage is the key determinant of FFR, we estimated the Ca^{2+} content by rapidly infusing caffeine after pacing the myocytes. Although increasing the pacing augmented the SR Ca^{2+} content in both NOS1$^{-/-}$ and WT CMs ($p < 0.05$, Table 1), the increase was smaller in NOS1$^{-/-}$ (38.2%) than WT (66.6%), which was consistent with previous studies (25). In the presence of HYD, NOS1$^{-/-}$ CMs also exhibited a rise in SR Ca^{2+} content in response to increasing frequency ($p < 0.05$, data not shown). SR Ca^{2+} content evaluated at 4 Hz was increased by HYD in a concentration-dependent manner, reaching a load similar to WT CMs ($p < 0.01$) (Fig. 4*H*). We also determined that, similar to HYD alone, the combination of equal concentrations of NTG and HYD increased the SR Ca^{2+} load in a concentration-dependent manner in NOS1$^{-/-}$ CMs (Fig. 4*H*). However, 10 μM HYD alone or combined with 10 μM NTG abolished the frequency-induced rise in SR Ca^{2+} content in WT CMs ($p = 0.001$ and $p = 0.005$, respectively; data not shown). NTG alone did not affect the SR Ca^{2+} load in NOS1$^{-/-}$ (Fig. 4*H*) or WT myocytes (data not shown).

Detection of Superoxide by DHE Staining—To determine the molecular underpinnings for improved E-C coupling in NOS1$^{-/-}$ myocytes in response to these drugs, we used the superoxide-sensitive dye DHE to assess the scavenging capacity of HYD and NTG alone, or in combination at 0.1, 1, or 10 μM (Fig. 5, *A* and *B*). As DHE is oxidized by superoxide and then translocated to the nucleus (Fig. 5*B*), the ratio between fluorescence in the nucleus and cytoplasm indexes superoxide production. Although the lowest drug concentrations did not affect superoxide detection, increasing concentrations of HYD as well as NTG scavenged superoxide ($p < 0.05$; Fig. 5*A*). In combination they had an additive effect ($p < 0.01$; Fig. 5*A*). Thus, at concentrations that reduced the SR Ca^{2+} leak, HYD alone or in combination with NTG exhibited an antioxidant effect.

NOX-dependent Superoxide Production—We also studied activation of specific oxidases, XOR and NOX, in mouse heart homogenates in the presence of either HYD or NTG. NOX activity of WT ($n = 3$) and NOS1$^{-/-}$ ($n = 4$) hearts was similar (2.29 ± 0.15 *versus* 2.19 ± 0.13 integrated light units/μg of protein, respectively). HYD (0.1–1 mM, IC_{50} 0.42 ± 0.23 mM) decreased NOX activity (Fig. 5*C*, $p < 0.01$ for both concentrations *versus* control) in NOS1$^{-/-}$ cardiac homogenates. NTG (>0.01 mM, IC_{50} 0.013 ± 0.06 mM) also inhibited NOX-dependent superoxide production (Fig. 5*C*; $p < 0.05$ for 0.01 mM, $p <$ 0.01 for 0.1 and 1 mM *versus* control).

XOR Activity—NOS1$^{-/-}$ hearts ($n = 3$) exhibited up-regulated XOR activity compared with WT ($n = 3$) using the Amplex Red detection of XOR-mediated ROS production assay (Fig. 5*D*; 2.1 ± 0.18 *versus* 1.63 ± 0.09 milliunits/μg of protein, respectively; $p < 0.05$), confirming previous findings in this mouse (25–27). Amplex Red XOR activity was inhibited by allopurinol (>0.01 mM, IC_{50} 0.19 ± 0.06 mM, Fig. 5*D*; $n = 3$) and HYD (IC_{50} of 0.7 ± 0.3 mM, Fig. 5*E*; $n = 3$) in NOS1$^{-/-}$ cardiac homogenates. Interestingly, NTG (IC_{50} 1.0 ± 0.4 mM, Fig. 5*E*, $n = 3$) also inhibited XOR. Because the Amplex Red assay

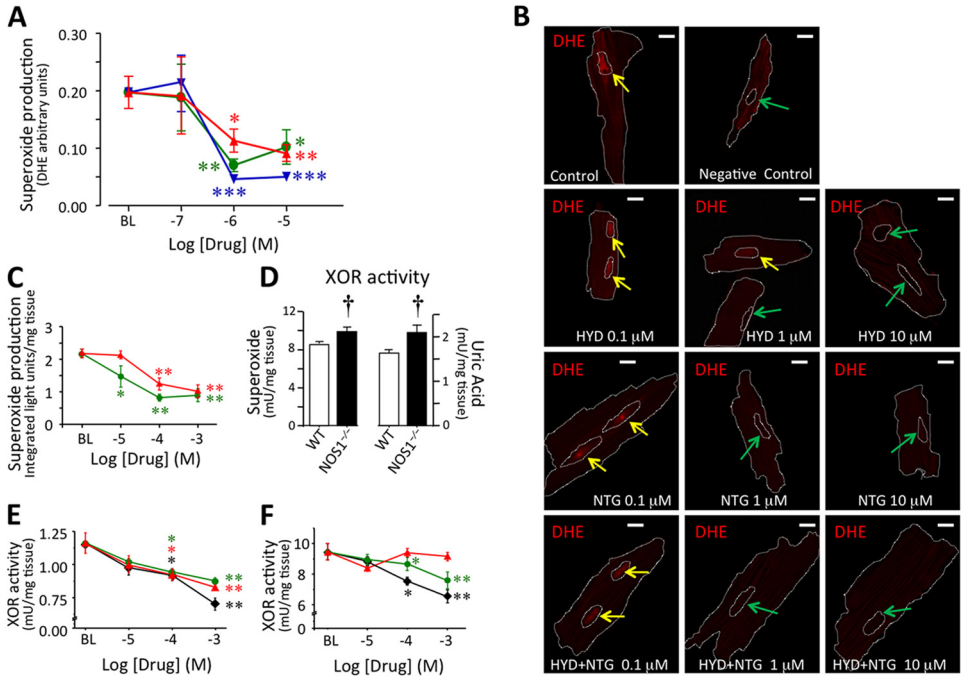

FIGURE 5. **Oxidative stress is attenuated by hydralazine and nitroglycerin.** *A*, superoxide-mediated oxidation of DHE. The ratio of fluorescence in the nucleus/cytoplasm preincubated 30 min with HYD (*red* ▲), NTG (*green* ●) and a combination of HYD + NTG (*blue* ▼) is shown. *B*, representative pictures of mice ventricular CMs stained with 3 μM DHE (superoxide-sensitive dye) in the absence (control) or presence (0.1, 1, or 10 μM) of the drugs (*Bar*, 10 μm). *Yellow arrows* indicate nuclei highly stained and *green arrows* show nuclei with little or no dye. *C*, NOX-dependent superoxide production in NOS1$^{-/-}$ cardiac homogenates. Effects of HYD and NTG on the NOX enzymatic system containing 0.3 mM NADPH as substrate. *D*, XOR activity in WT and NOS1$^{-/-}$ mouse hearts in terms of superoxide production (*left*) or uric acid generation (*right*). *E*, effect of allopurinol (◆), HYD, and NTG on XOR-dependent superoxide production in NOS1$^{-/-}$ cardiac homogenates. *F*, effects of allopurinol, HYD, and NTG on uric acid production in the XOR enzymatic system containing 0.2 mM xanthine as substrate. *, $p < 0.05$; **, $p < 0.01$; and ***, $p < 0.001$ *versus* baseline, one-way ANOVA; †, $p < 0.05$ *versus* nontreated NOS1$^{-/-}$, Student's *t* test.

measures superoxide levels, reduced activity could also reflect increased O_2^- scavenging. To address this possibility, we measured uric acid conversion as a direct measurement of enzymatic activity. With this approach, NOS1$^{-/-}$ hearts ($n = 3$) again exhibited increased XOR activity compared with WT ($n = 3$) (Fig. 5*D*; 9.8 ± 0.46 *versus* 8.5 ± 0.21 milliunits/mg tissue, respectively, $p < 0.05$). Allopurinol (>0.1 mM) inhibited XOR enzyme activity in NOS1$^{-/-}$ mice (Fig. 5*F*, $n = 3$). Interestingly, HYD did not, but NTG did display XOR-inhibitory activity in NOS1$^{-/-}$ (Fig. 5*F*, $n = 3$).

Organic Nitrates Increased Myofilament Responsiveness to Ca^{2+} in NOS1$^{-/-}$ Myocytes—Because our FFR data suggested that organic nitrates improve efficiency in myofilament responsiveness to $Ca^{2+}{}_i$, we assessed the mechanism by which NTG offsets the HYD-induced $\Delta[Ca^{2+}]_i$ increase toward normal, and directly tested the myofilament responsiveness in NOS1$^{-/-}$ as well as WT CMs in the presence of 10 μM NTG. Responsiveness of myofilaments to Ca^{2+} (both sensitivity and maximal response) was lower in NOS1$^{-/-}$ compared with WT CMs ($EC_{50,NOS1-/-} = 0.627 \pm 0.0185$ and $EC_{50,WT} = 0.398 \pm 0.018$ μM, respectively; $p = 0.0009$, Fig. 6, *A–D*). In agreement with previous studies using different NO donors (23, 28), NTG reduced myofilament responsiveness to $Ca^{2+}{}_i$ in WT (not shown). Surprisingly, but consistent with our results, NTG increased responsiveness to Ca^{2+} in NOS1$^{-/-}$ (Fig. 6, *B* and *D*), as shown by a leftward shift ($EC_{50,NOS1-/-,NTG} = 0.427 \pm 0.0186$ μM, $p = 0.0016$; Fig. 6*C*). Therefore, NTG restored the impaired myofilament sensitivity in NOS1$^{-/-}$ toward normal levels observed in WT CMs. Analysis of $[Ca^{2+}]_i$-SL shortening loops confirm that sensitivity to Ca^{2+} is deficient in NOS1$^{-/-}$ CMs but treatment with 10 μM ISDN improves it toward WT (Fig. 6*E*).

Frequency-stimulated Contractility and Ca^{2+} Transients Are Improved by Hydralazine and Nitroglycerin in CMs from Heart Failure Rats—To study the effects of HYD and NTG in a model of heart failure (dilated cardiomyopathy), we used SHHF rats. Usually, the SL shortening amplitude in rat CMs is flat or negative in response to increasing the pacing rate. We recently showed that SL shortening drops more abruptly in SHHF than WKY control CMs (13). Here, we also observed a significant decrease in contractility in SHHF compared with WKY CMs ($p = 0.0002$, Fig. 7, *A* and *B*). Treatment with 10 μM HYD significantly improved SL shortening in SHHF myocytes ($p = 0.0414$). Consistent with observations in NOS1$^{-/-}$, 10 μM NTG did not affect the SL shortening in SHHF myocytes ($p = 0.2553$). The combination of HYD and NTG showed a strong trend toward increased contractility in SHHF myocytes ($p = 0.0839$), which also exhibited an FFR pattern similar to HYD alone (Fig. 7*A*). Furthermore, there was a significant difference at 4 Hz compared with the SHHF control ($p = 0.0359$, Fig. 7*B*). Normalization of SL shortening as a percentage of 0.5 Hz pacing showed that HYD alone as well as in combination with NTG significantly improved FFR in failing CMs ($p = 0.035$ and $p = 0.0013$, respectively, data not shown).

The ΔCa^{2+} increased in WKY CMs in response to pacing ($p = 0.0019$, Fig. 7*C*), compared with the flat pattern in SHHF CMs. In agreement with the results obtained in NOS1$^{-/-}$ mice, in failing CMs $\Delta[Ca^{2+}]_i$ amplitude was augmented by 10 μM

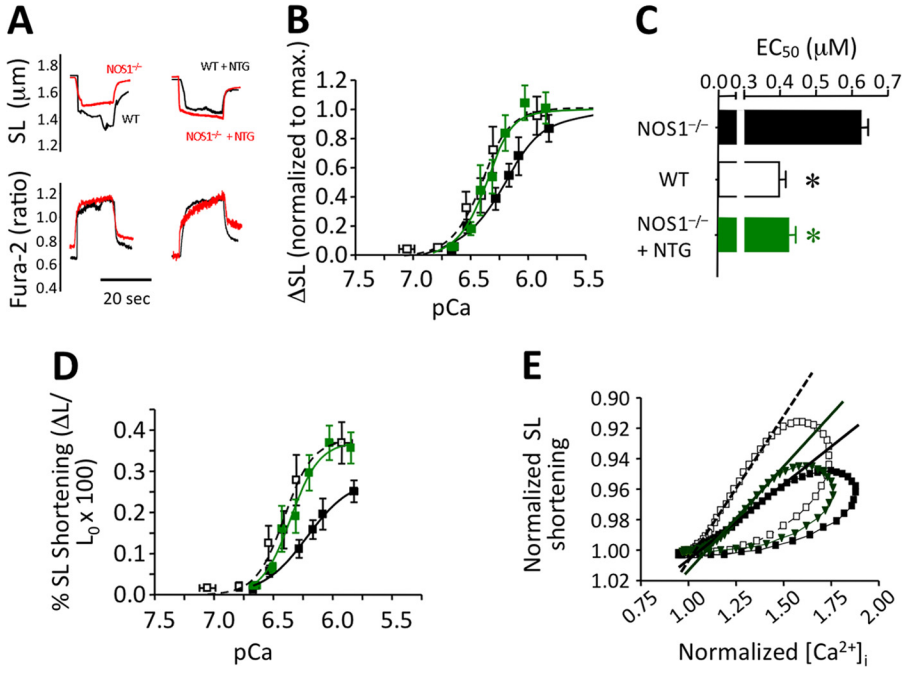

FIGURE 6. **Myofilament sensitivity to Ca^{2+} in $NOS1^{-/-}$ cardiomyocytes.** *A*, representative traces of SL shortening (*top*) in response to similar increases of $Ca^{2+}{}_i$ (*bottom*) obtained by high frequency-induced tetanus of the CMs in the presence of thapsigargin. Response of $NOS1^{-/-}$ was compared with WT cells in the absence (*left*) or presence of 10 μM NTG (*right*). *B*, curves of myofilament sensitivity to $[Ca^{2+}]_i$ in $NOS1^{-/-}$ baseline (■) or 10 μM NTG-treated (*green* ■) CMs compared with WT (□) as normalized to the maximal response in each group (sigmoidal dose-response − variable slope − fitting). *C*, EC_{50} values of the curves. *D*, myofilament sensitivity curves expressed as absolute values; the fitting provides not only higher EC_{50} values but also a smaller maximal response in the $NOS1^{-/-}$ control. *E*, SL shortening − $[Ca^{2+}]_i$ loops of WT (□; $n = 27$ cells) or $NOS1^{-/-}$ CMs in the absence (■; $n = 30$ cells) or presence of 10 μM ISDN (*dark green* ▼; $n = 10$ cells). The slopes that fit the relaxation phases of the loops correlate with the sensitivity of myofilaments to Ca^{2+}. Sensitivity of $NOS1^{-/-}$ (—) is lower than WT (- - -); however, treatment with ISDN (—) increased the fitted slope toward the values observed in WT CMs. *, $p < 0.05$ *versus* $NOS1^{-/-}$, Student's *t* test.

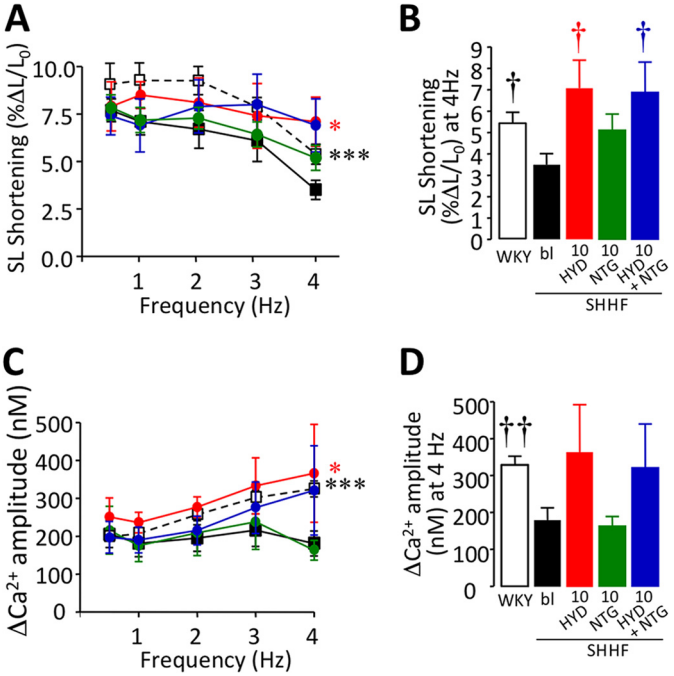

FIGURE 7. **SL shortening and Ca^{2+} transient amplitude-frequency response in SHHF cardiomyocytes.** *A*, FFR in SHHF rat CMs in the absence (■) or presence of 10 μM HYD (*red* ●), 10 μM NTG (*green* ●), or a combination (HYD + NTG, 10 μM each; *blue* ●) compared with WKY control CMs (□). *B*, bar graph showing contractility data at 4 Hz. *C*, Ca^{2+}-FFR in SHHF rat CMs treated with 10 μM HYD or 10 μM NTG or their combination (HYD + NTG, 10 μM each). *D*, bar graph showing $\Delta[Ca^{2+}]_i$ data at 4 Hz. In SHHF CMs, similar effects to those observed in $NOS1^{-/-}$ were obtained with these treatments ($n = 5$–15 cells). *, $p < 0.05$; ***, $p < 0.001$ *versus* SHHF control; two-way ANOVA. †, $p < 0.05$; ††, $p < 0.01$ *versus* SHHF control, Student's *t* test.

HYD ($p = 0.0124$) in comparison to SHHF controls (Fig. 7*C*). In this setting, the combination of HYD with 10 μM NTG also induced a nonsignificant rise in $\Delta[Ca^{2+}]_i$ primarily at the highest frequency ($p = 0.1756$, Fig. 7*D*). On the other hand, consistent with the effect observed in contractility in this model, $\Delta[Ca^{2+}]_i$ was not affected by NTG (Fig. 7, *C* and *D*). Therefore treatment with HYD and NTG in a genetic model of heart failure enhances E-C coupling in a similar fashion (yet species appropriate) as observed in $NOS1^{-/-}$ cells, a model of NO/redox imbalance.

DISCUSSION

Our major new finding is that HYD and NTG corrected the increased Ca^{2+} leak from the SR, thus normalizing contractility-frequency responses by modulating Ca^{2+} cycling in models of NO/redox imbalance. Although HYD improved contractile force in parallel with increasing Ca^{2+} transients and total restoration of leak, NTG offset Ca^{2+} cycling without impairing contractility, thereby improving contractile efficiency. Direct measure of myofilament sensitivity confirmed that NTG restores depressed myofilament sensitivity to Ca^{2+} in $NOS1^{-/-}$ myocytes. Importantly, NTG inhibited two major sources of cellular ROS production, NOX and XOR, and also exhibited ROS scavenging capacity. HYD scavenged ROS but did not inhibit XOR. Although NOX activity appeared to be inhibited by HYD, this effect could be an epiphenomenon due to the superoxide scavenging properties of HYD, because NOX activity was only assessed by NADPH-induced superoxide production. Despite the lack of NOS1-derived NO and the fact that NOS3 is uncoupled under oxidative stress (29), peroxynitrite

($ONOO^-$) was measurable in $NOS1^{-/-}$ homogenates and was reduced by both HYD and NTG, in a dose-dependent manner (data not shown).

Model of NO-Redox Imbalance—$NOS1^{-/-}$ mice are widely used to investigate the involvement of NO in E-C coupling because CMs exhibit a particularly impaired performance due to deficient NO production and consequent NO/redox imbalance (12, 25). Sears *et al.* (30) showed that $NOS1^{-/-}$ CMs have larger ΔCa^{2+}, which is consistent with larger I_{Ca} and augmented SL shortening compared with control animals, at low frequencies. However, we (12, 18) and others (31) have shown that the contractile reserve is impaired in $NOS1^{-/-}$ as the increase in ΔCa^{2+} and contractility in response to pacing are depressed. Consistently, we have found that the reduced SR Ca^{2+} load was associated with augmented SR Ca^{2+} leak. In contrast, Sears *et al.* (30) found that the SR Ca^{2+} load was higher in $NOS1^{-/-}$, when measured at 1 Hz. In our hands, SR Ca^{2+} loads at low frequencies were not different between strains, but during pacing with rates more physiologic for murine myocytes, were depressed *versus* WT (25). Similarly, Wang and colleagues (32) demonstrated that the SR Ca^{2+} leak is reduced in $NOS1^{-/-}$ myocytes, suggesting that NOS1-derived NO induces RyR2 to leak. However, and in contrast to our experiments, this group studied the SR Ca^{2+} leak at room temperature (22 °C), whereas, we assessed the leak at 37 °C. This simple detail may be responsible for the differences. We recently demonstrated that SHHF rats, a representative heart failure model that exhibits oxidative stress as a hallmark (13), share certain specific features with $NOS1^{-/-}$ mice. Both models exhibit increased superoxide production associated with elevated XOR activity (25) and blunted NOS1 activity, evidenced by hyponitrosylation of RyR2 (12). Moreover, increased SR Ca^{2+} leak, reduced SR Ca^{2+} load, and depressed Ca^{2+} and force-frequency responses are characteristics of these models (13, 18). Unlike SHHF rats, $NOS1^{-/-}$ mice are not considered a representative model for heart failure. Rather, they develop age-related cardiac hypertrophy (a pre-heart failure stage) and exhibit accelerated mortality (33, 34). Additionally, after myocardial infarction, $NOS1^{-/-}$ also undergo exaggerated remodeling and higher mortality than WT controls (27). Consequently, $NOS1^{-/-}$ mice are an excellent model of NO/redox imbalance that share features with a model of heart failure, the SHHF rat.

Therapeutic Use of Hydralazine and Organic Nitrates—Recently, Cole *et al.* (2) reviewed the use of HYD-ISDN as a treatment for heart failure (1, 3) highlighting the fact that the mechanistic basis for this regimen to reduce all-cause mortality remains to be established. We show for the first time that this regimen restores disrupted NO/redox equilibrium and in so doing restores E-C coupling derangements.

The effects of HYD and NTG resemble, in part, those of XOR inhibitors. Allopurinol improves myocyte contraction without changing $\Delta[Ca^{2+}]_i$ enhancing contractile efficiency in both $NOS1^{-/-}$ mice and heart failure models (25, 35, 36). In large animal models, allopurinol restores mechano-energetic uncoupling (15). Interestingly, XOR inhibitors did not have clinical benefits in a broad heart failure population, although it may improve outcomes in patients with high uric acid levels (37) and may benefit patients with hypertension and ischemic heart disease (38–40).

Mechanism of Action and Pharmacology of Hydralazine—HYD is a peripheral vasodilator used for decades to treat essential hypertension and heart failure. The mechanism of its effect on the vasculature remains unknown. It is proposed to inhibit the endoplasmic reticulum Ca^{2+} release in vascular smooth muscle (41, 42), although the molecular mechanism by which HYD regulates the IP_3 receptor (a member of the superfamily of homotetrameric ligand-gated intracellular Ca^{2+} channels, which includes RyR2) has not been elucidated. Because HYD increases contractility and Ca^{2+} transients in myocardial fibers (43), it may positively affect the unregulated RyR2 activity in $NOS1^{-/-}$.

We showed that HYD enhanced depressed $NOS1^{-/-}$ CM contractility and $[Ca^{2+}]_i$ responses resulting from NO/redox imbalance. Importantly, HYD restored the increased SR Ca^{2+} leakage both alone or in combination with NTG. This feature suggests a regulatory action of HYD on RyR2 gating, possibly depressing Ca^{2+} release in diastole and enhancing gating in systole.

Accordingly, a more efficient handling of Ca^{2+} would underlie the recovery of the SR Ca^{2+} content observed in CMs treated with HYD or HYD plus NTG. Biochemically, HYD + NTG exhibited an additive superoxide scavenging capacity at concentrations as low as 1 μM, as shown by DHE staining. This effect may be correlated with the additive acceleration in SR Ca^{2+} reuptake in $NOS1^{-/-}$ induced by combining HYD with NTG. Peroxynitrite links superoxide production to Ca^{2+} reuptake. Although $ONOO^-$ generation depends on superoxide availability, PLB phosphorylation is decreased due to $ONOO^-$-dependent activation of phosphatases, impairing Ca^{2+} decay and relaxation in $NOS1^{-/-}$ (31, 44, 45). Furthermore, HYD and NTG scavenged $ONOO^-$ in $NOS1^{-/-}$ heart homogenates (data not shown). Together these findings suggest a role for scavenging of $ONOO^-$ on the recovery of the Ca^{2+} reuptake rate, a key process in E-C coupling in mouse CMs (44, 46). Considerable evidence supports the hypothesis that oxidative stress induces cardiac injury by oxidizing cellular constituents, including proteins critical for E-C coupling, and largely by diminishing NO bioactivity (9), thus playing a role in heart failure pathophysiology (47). Therefore, the effect of HYD, which reduced $ONOO^-$ in $NOS1^{-/-}$ hearts (data not shown), and scavenged XOR-mediated superoxide production may impact the redox regulation of RyR2 gating and the pharmacology of the response. Importantly, our results agree with Leiro *et al.* (48), who suggested antioxidant properties for HYD.

Mechanism of Action and Pharmacology of Organic Nitrates—Janero *et al.* (49) showed that NTG increases cardiac nitrosylation *in vivo*, and this effect was potentiated by xanthine oxidase inhibition with allopurinol, highlighting the interactions between NO and XOR-derived superoxide. Importantly, decreased NOS1 in cardiac SR contributes to depressed contractile reserve in response to pacing. It has been hypothesized that NTG may restore ion channel *S*-nitrosylation in $NOS1^{-/-}$ myocytes (24). We showed that NTG and ISDN restored the normal amplitude of calcium transients toward WT levels in $NOS1^{-/-}$ cells treated with HYD. This effect would be consis-

tent with a cGMP-dependent regulation of L-type Ca^{2+} channels and/or restoration of RyR2 *S*-nitrosylation (33, 50) and occurs without affecting cardiac contractility, which correlates with the observed improvement in myofilament sensitivity induced by NTG in NOS1$^{-/-}$ CMs. This improvement may also be attributed to the restoration of the *S*-nitrosylation/normal redox state of redox-sensitive sites on sarcomeric proteins. Thus, this responsiveness is evident across the broad range of pacing frequencies tested, confirming that organic nitrates enhance contractile efficiency. It is reasonable to speculate that the lack of NOS1 and the resulting NO/redox imbalance reduces responsiveness of myofilaments to Ca^{2+} (as confirmed by our results). This reduction was restored by NO donors. These findings suggest that a feasible mechanism for the positive clinical outcomes of organic nitrates (when combined with HYD) may be by regulating intracellular Ca^{2+} handling and restoring myofilament sensitivity impaired by NO/redox imbalance, thereby modulating E-C coupling toward a more efficient performance.

Inhibition of NOX and XOR by NO has been previously demonstrated (26, 51–53), supporting our results. In contrast to the low concentrations required to scavenge superoxide production in isolated myocytes, the effective concentrations of NTG to inhibit the substrate-induced activity of these enzymes in cardiac homogenates exceeded achievable blood levels of this drug (10 ng/ml, 44 nM) (54).

Despite the successful use of nitrates such as NTG or ISDN in the treatment of a variety of cardiovascular diseases, nitrate tolerance during long-term use in heart failure has been described. Co-treatment with HYD has been demonstrated to prevent this effect (55) and several authors have tried to explain the mechanism of this phenomenon (56–58).

The effects of organic nitrates on SR Ca^{2+} leak appear to be uncertain and depend strongly on several variants such as the concentration or nature of the NO donor. As shown in the supplemental material, NTG exerted differential effects along the range of concentrations from 0.1 to 100 μM. On the other hand, ISDN reduced the SR leak in NOS1$^{-/-}$ at very low SR Ca^{2+} contents but did not affect it at increasing Ca^{2+} loads. We speculate that this differential response may correspond to the delicate equilibrium of the nitrosylation/denitrosylation cycle involved in the regulation of RyR2 activity (50).

Combination of HYD and NTG—The effect of NTG in NOS1$^{-/-}$ hearts may appear puzzling. At lower concentrations (0.1 and 1 μM), NTG did not significantly affect SL shortening, Ca^{2+} transient, SR Ca^{2+} leak or Ca^{2+} decline. It reduced the Ca^{2+} frequency response with a concomitant acceleration of Ca^{2+} decline at 10 μM. However, despite 10 μM NTG improving Ca^{2+} reuptake, there was a trend toward increasing SR Ca^{2+} leak (or at least effecting no change on SR Ca^{2+} leak; Fig. 3*E*), which would counteract the improvement in Ca^{2+} influx by the SR, thereby abolishing the SR Ca^{2+} content recovery. This balancing may explain why there was no change in SR Ca^{2+} load, although this was not reflected on the Ca^{2+} amplitude, which was reduced. Because Ca^{2+} influx (I_{Ca}) was enhanced in NOS1$^{-/-}$ (30), the reduced RyR2 gating in the presence of 10 μM NTG (or ISDN) may be caused by the down-regulation of the enhanced I_{Ca} in NOS1$^{-/-}$ by exogenous NO (as previously shown) (24). Thus, whereas hydralazine alone reduced RyR2 leak, when combined with NTG (or ISDN), down-regulation of the Ca^{2+}-induced Ca^{2+} release (via inhibition of I_{Ca}) would oppose the effect of hydralazine, thereby leading to a reduced Ca^{2+} transient amplitude. Together with the reduced leak and increased reuptake under these conditions, the contractile reserve was recovered in NOS1$^{-/-}$. Thus, the evidence of improved EC coupling in this model using the HYD-NTG treatment would be restoration of Ca^{2+} levels toward those exhibited by WT CMs and recovery of the increasing Ca^{2+} frequency response and myofilament responsiveness to Ca^{2+}, where NTG played a key role.

Both HYD and NTG scavenged superoxide but were more potent in combination. However, we must consider that the chemical reactions of each molecule with superoxide yield different products. Although HYD can effectively scavenge the radical, the combination of NO and superoxide yields $ONOO^-$, a reactive nitrogen species even more harmful than superoxide. In this sense, we speculate that $ONOO^-$ may target RyR2 in a similar manner as superoxide. Therefore, the SR Ca^{2+} leak was still elevated in the presence of NTG. Fig. 4*F* showed that despite 10 μM NTG inducing a trend toward an increased leak in NOS1$^{-/-}$, 100 μM NTG restored it to baseline. This observation suggests that higher concentrations of NTG not only scavenge superoxide but also the surplus would counteract the deficiency of NO in NOS1$^{-/-}$ and is perhaps the mechanism of the combination of NTG and HYD.

Effects in SHHF Rats—Although this study is focused on NOS1$^{-/-}$ myocytes as a model of NO/redox imbalance, we also tested the effect of these drugs alone or in combination on failing CMs from SHHF rats. The results obtained in SHHF CMs correlate with those in NOS1$^{-/-}$ mice. HYD alone or in combination with NTG improved the Ca^{2+}-frequency response and FFR. NTG alone induced a trend to increase contractility at 4 Hz with no changes in ΔCa^{2+}, suggesting an improvement in myofilament sensitivity. These results allow us to speculate that our approach may be extrapolated to heart failure in humans.

Conclusion—Our data show novel effects of HYD and NTG. In combination they quench superoxide in isolated cells, concomitantly with physiologic functional effects, including improved myocardial contractility and Ca^{2+} cycling. At higher *in vitro* concentrations, this combination scavenges superoxide and peroxynitrite production from two major ROS generating enzymatic systems, NOX and XOR. This improvement in myocyte performance, normalization of SR Ca^{2+} leak, regulation of RyR2 gating, and myofilament sensitivity by NTG may be associated in part with normalizing NO/redox equilibrium. Thus, these drugs in combination exert direct myocardial effects that provide a mechanistic basis for the favorable functional and structural responses in the treatment of congestive heart failure.

Acknowledgments—We thank Drs. Ivonne Schulman and Wayne Balkan for critical reading of the manuscript.

REFERENCES

1. Taylor, A. L., Ziesche, S., Yancy, C., Carson, P., D'Agostino, R., Jr., Ferdinand, K., Taylor, M., Adams, K., Sabolinski, M., Worcel, M., and Cohn,

J. N. (2004) Combination of isosorbide dinitrate and hydralazine in blacks with heart failure. *N. Engl. J. Med.* **351,** 2049–2057
2. Cole, R. T., Kalogeropoulos, A. P., Georgiopoulou, V. V., Gheorghiade, M., Quyyumi, A., Yancy, C., and Butler, J. (2011) Hydralazine and isosorbide dinitrate in heart failure. Historical perspective, mechanisms, and future directions. *Circulation* **123,** 2414–2422
3. Taylor, A. L., Sabolinski, M. L., Tam, S. W., Ziesche, S., Ghali, J. K., Archambault, W. T., Worcel, M., and Cohn, J. N. (2012) Effect of fixed-dose combined isosorbide dinitrate/hydralazine in elderly patients in the African-American heart failure trial. *J. Card. Fail.* **18,** 600–606
4. Antoons, G., Vangheluwe, P., Volders, P. G., Bito, V., Holemans, P., Ceci, M., Wuytack, F., Caroni, P., Mubagwa, K., and Sipido, K. R. (2006) Increased phospholamban phosphorylation limits the force-frequency response in the $MLP^{-/-}$ mouse with heart failure. *J. Mol. Cell Cardiol.* **40,** 350–360
5. Lamberts, R. R., Hamdani, N., Soekhoe, T. W., Boontje, N. M., Zaremba, R., Walker, L. A., de Tombe, P. P., van der Velden, J., and Stienen, G. J. (2007) Frequency-dependent myofilament Ca^{2+} desensitization in failing rat myocardium. *J. Physiol.* **582,** 695–709
6. Rossman, E. I., Petre, R. E., Chaudhary, K. W., Piacentino, V., 3rd, Janssen, P. M., Gaughan, J. P., Houser, S. R., and Margulies, K. B. (2004) Abnormal frequency-dependent responses represent the pathophysiologic signature of contractile failure in human myocardium. *J. Mol. Cell Cardiol.* **36,** 33–42
7. O'Rourke, B., Kass, D. A., Tomaselli, G. F., Kääb, S., Tunin, R., and Marbán, E. (1999) Mechanisms of altered excitation-contraction coupling in canine tachycardia-induced heart failure. I: experimental studies. *Circ. Res.* **84,** 562–570
8. Yano, M., Ikeda, Y., and Matsuzaki, M. (2005) Altered intracellular Ca^{2+} handling in heart failure. *J. Clin. Invest.* **115,** 556–564
9. Hare, J. M. (2004) Nitroso-redox balance in the cardiovascular system. *N. Engl. J. Med.* **351,** 2112–2114
10. Hare, J. M., and Stamler, J. S. (2005) NO/redox disequilibrium in the failing heart and cardiovascular system. *J. Clin. Invest.* **115,** 509–517
11. Terentyev, D., Györke, I., Belevych, A. E., Terentyeva, R., Sridhar, A., Nishijima, Y., de Blanco, E. C., Khanna, S., Sen, C. K., Cardounel, A. J., Carnes, C. A., and Györke, S. (2008) Redox modification of ryanodine receptors contributes to sarcoplasmic reticulum Ca^{2+} leak in chronic heart failure. *Circ. Res.* **103,** 1466–1472
12. Gonzalez, D. R., Beigi, F., Treuer, A. V., and Hare, J. M. (2007) Deficient ryanodine receptor *S*-nitrosylation increases sarcoplasmic reticulum calcium leak and arrhythmogenesis in cardiomyocytes. *Proc. Natl. Acad. Sci. U.S.A.* **104,** 20612–20617
13. Gonzalez, D. R., Treuer, A. V., Castellanos, J., Dulce, R. A., and Hare, J. M. (2010) Impaired *S*-nitrosylation of the ryanodine receptor caused by xanthine oxidase activity contributes to calcium leak in heart failure. *J. Biol. Chem.* **285,** 28938–28945
14. Cappola, T. P., Kass, D. A., Nelson, G. S., Berger, R. D., Rosas, G. O., Kobeissi, Z. A., Marbán, E., and Hare, J. M. (2001) Allopurinol improves myocardial efficiency in patients with idiopathic dilated cardiomyopathy. *Circulation* **104,** 2407–2411
15. Saavedra, W. F., Paolocci, N., St John, M. E., Skaf, M. W., Stewart, G. C., Xie, J. S., Harrison, R. W., Zeichner, J., Mudrick, D., Marbán, E., Kass, D. A., and Hare, J. M. (2002) Imbalance between xanthine oxidase and nitric-oxide synthase signaling pathways underlies mechanoenergetic uncoupling in the failing heart. *Circ. Res.* **90,** 297–304
16. Saraiva, R. M., Minhas, K. M., Zheng, M., Pitz, E., Treuer, A., Gonzalez, D., Schuleri, K. H., Vandegaer, K. M., Barouch, L. A., and Hare, J. M. (2007) Reduced neuronal nitric oxide synthase expression contributes to cardiac oxidative stress and nitroso-redox imbalance in ob/ob mice. *Nitric. Oxide.* **16,** 331–338
17. Tziomalos, K., and Hare, J. M. (2009) Role of xanthine oxidoreductase in cardiac nitroso-redox imbalance. *Front. Biosci.* **14,** 237–262
18. Khan, S. A., Skaf, M. W., Harrison, R. W., Lee, K., Minhas, K. M., Kumar, A., Fradley, M., Shoukas, A. A., Berkowitz, D. E., and Hare, J. M. (2003) Nitric oxide regulation of myocardial contractility and calcium cycling. Independent impact of neuronal and endothelial nitric oxide synthases. *Circ. Res.* **92,** 1322–1329
19. Grynkiewicz, G., Poenie, M., and Tsien, R. Y. (1985) A new generation of Ca^{2+} indicators with greatly improved fluorescence properties. *J. Biol. Chem.* **260,** 3440–3450
20. Shannon, T. R., Ginsburg, K. S., and Bers, D. M. (2002) Quantitative assessment of the SR Ca^{2+} leak-load relationship. *Circ. Res.* **91,** 594–600
21. Bassani, R. A., Bassani, J. W., and Bers, D. M. (1992) Mitochondrial and sarcolemmal Ca^{2+} transport reduce $[Ca^{2+}]_i$ during caffeine contractures in rabbit cardiac myocytes. *J. Physiol.* **453,** 591–608
22. Robak, J., and Gryglewski, R. J. (1988) Flavonoids are scavengers of superoxide anions. *Biochem. Pharmacol.* **37,** 837–841
23. Vila-Petroff, M. G., Younes, A., Egan, J., Lakatta, E. G., and Sollott, S. J. (1999) Activation of distinct cAMP-dependent and cGMP-dependent pathways by nitric oxide in cardiac myocytes. *Circ. Res.* **84,** 1020–1031
24. Burger, D. E., Lu, X., Lei, M., Xiang, F. L., Hammoud, L., Jiang, M., Wang, H., Jones, D. L., Sims, S. M., and Feng, Q. (2009) Neuronal nitric-oxide synthase protects against myocardial infarction-induced ventricular arrhythmia and mortality in mice. *Circulation* **120,** 1345–1354
25. Khan, S. A., Lee, K., Minhas, K. M., Gonzalez, D. R., Raju, S. V., Tejani, A. D., Li, D., Berkowitz, D. E., and Hare, J. M. (2004) Neuronal nitric-oxide synthase negatively regulates xanthine oxidoreductase inhibition of cardiac excitation-contraction coupling. *Proc. Natl. Acad. Sci. U.S.A.* **101,** 15944–15948
26. Kinugawa, S., Huang, H., Wang, Z., Kaminski, P. M., Wolin, M. S., and Hintze, T. H. (2005) A defect of neuronal nitric oxide synthase increases xanthine oxidase-derived superoxide anion and attenuates the control of myocardial oxygen consumption by nitric oxide derived from endothelial nitric oxide synthase. *Circ. Res.* **96,** 355–362
27. Saraiva, R. M., Minhas, K. M., Raju, S. V., Barouch, L. A., Pitz, E., Schuleri, K. H., Vandegaer, K., Li, D., and Hare, J. M. (2005) Deficiency of neuronal nitric oxide synthase increases mortality and cardiac remodeling after myocardial infarction. Role of nitroso-redox equilibrium. *Circulation* **112,** 3415–3422
28. Layland, J., Li, J. M., and Shah, A. M. (2002) Role of cyclic GMP-dependent protein kinase in the contractile response to exogenous nitric oxide in rat cardiac myocytes. *J. Physiol.* **540,** 457–467
29. Chen, C. A., Wang, T. Y., Varadharaj, S., Reyes, L. A., Hemann, C., Talukder, M. A., Chen, Y. R., Druhan, L. J., and Zweier, J. L. (2010) *S*-Glutathionylation uncouples eNOS and regulates its cellular and vascular function. *Nature* **468,** 1115–1118
30. Sears, C. E., Bryant, S. M., Ashley, E. A., Lygate, C. A., Rakovic, S., Wallis, H. L., Neubauer, S., Terrar, D. A., and Casadei, B. (2003) Cardiac neuronal nitric-oxide synthase isoform regulates myocardial contraction and calcium handling. *Circ. Res.* **92,** e52-e59
31. Wang, H., Kohr, M. J., Traynham, C. J., Wheeler, D. G., Janssen, P. M., and Ziolo, M. T. (2008) Neuronal nitric-oxide synthase signaling within cardiac myocytes targets phospholamban. *Am. J. Physiol. Cell Physiol.* **294,** C1566-C1575
32. Wang, H., Viatchenko-Karpinski, S., Sun, J., Györke, I., Benkusky, N. A., Kohr, M. J., Valdivia, H. H., Murphy, E., Györke, S., and Ziolo, M. T. (2010) Regulation of myocyte contraction via neuronal nitric oxide synthase. Role of ryanodine receptor *S*-nitrosylation. *J. Physiol.* **588,** 2905–2917
33. Barouch, L. A., Harrison, R. W., Skaf, M. W., Rosas, G. O., Cappola, T. P., Kobeissi, Z. A., Hobai, I. A., Lemmon, C. A., Burnett, A. L., O'Rourke, B., Rodriguez, E. R., Huang, P. L., Lima, J. A., Berkowitz, D. E., and Hare, J. M. (2002) Nitric oxide regulates the heart by spatial confinement of nitric-oxide synthase isoforms. *Nature* **416,** 337–339
34. Barouch, L. A., Cappola, T. P., Harrison, R. W., Crone, J. K., Rodriguez, E. R., Burnett, A. L., and Hare, J. M. (2003) Combined loss of neuronal and endothelial nitric-oxide synthase causes premature mortality and age-related hypertrophic cardiac remodeling in mice. *J. Mol. Cell Cardiol.* **35,** 637–644
35. Amado, L. C., Saliaris, A. P., Raju, S. V., Lehrke, S., St John, M., Xie, J., Stewart, G., Fitton, T., Minhas, K. M., Brawn, J., and Hare, J. M. (2005) Xanthine oxidase inhibition ameliorates cardiovascular dysfunction in dogs with pacing-induced heart failure. *J. Mol. Cell Cardiol.* **39,** 531–536
36. Ekelund, U. E., Harrison, R. W., Shokek, O., Thakkar, R. N., Tunin, R. S., Senzaki, H., Kass, D. A., Marbán, E., and Hare, J. M. (1999) Intravenous allopurinol decreases myocardial oxygen consumption and increases me-

chanical efficiency in dogs with pacing-induced heart failure. *Circ. Res.* **85,** 437–445
37. Hare, J. M., Mangal, B., Brown, J., Fisher, C., Jr., Freudenberger, R., Colucci, W. S., Mann, D. L., Liu, P., Givertz, M. M., and Schwarz, R. P. (2008) Impact of oxypurinol in patients with symptomatic heart failure. Results of the OPT-CHF study. *J. Am. Coll. Cardiol.* **51,** 2301–2309
38. Bergamini, C., Cicoira, M., Rossi, A., and Vassanelli, C. (2009) Oxidative stress and hyperuricaemia. Pathophysiology, clinical relevance, and therapeutic implications in chronic heart failure. *Eur. J. Heart Fail.* **11,** 444–452
39. Noman, A., Ang, D. S., Ogston, S., Lang, C. C., and Struthers, A. D. (2010) Effect of high-dose allopurinol on exercise in patients with chronic stable angina. A randomised, placebo controlled crossover trial. *Lancet* **375,** 2161–2167
40. Zoccali, C., Maio, R., Mallamaci, F., Sesti, G., and Perticone, F. (2006) Uric acid and endothelial dysfunction in essential hypertension. *J. Am. Soc. Nephrol.* **17,** 1466–1471
41. Gurney, A. M., and Allam, M. (1995) Inhibition of calcium release from the sarcoplasmic reticulum of rabbit aorta by hydralazine. *Br. J. Pharmacol.* **114,** 238–244
42. Ellershaw, D. C., and Gurney, A. M. (2001) Mechanisms of hydralazine induced vasodilation in rabbit aorta and pulmonary artery. *Br. J. Pharmacol.* **134,** 621–631
43. Miao, L., Perreault, C. L., Travers, K. E., and Morgan, J. P. (1997) Mechanisms of positive inotropic action of flosequinan, hydralazine, and milrinone on mammalian myocardium. *Eur. J. Pharmacol.* **321,** 201–208
44. Kohr, M. J., Wang, H., Wheeler, D. G., Velayutham, M., Zweier, J. L., and Ziolo, M. T. (2008) Targeting of phospholamban by peroxynitrite decreases β-adrenergic stimulation in cardiomyocytes. *Cardiovasc. Res.* **77,** 353–361
45. Zhang, Y. H., Zhang, M. H., Sears, C. E., Emanuel, K., Redwood, C., El-Armouche, A., Kranias, E. G., and Casadei, B. (2008) Reduced phospholamban phosphorylation is associated with impaired relaxation in left ventricular myocytes from neuronal NO synthase-deficient mice. *Circ. Res.* **102,** 242–249
46. Katori, T., Donzelli, S., Tocchetti, C. G., Miranda, K. M., Cormaci, G., Thomas, D. D., Ketner, E. A., Lee, M. J., Mancardi, D., Wink, D. A., Kass, D. A., and Paolocci, N. (2006) Peroxynitrite and myocardial contractility. *In vivo versus in vitro* effects. *Free Radic. Biol. Med.* **41,** 1606–1618
47. Giordano, F. J. (2005) Oxygen, oxidative stress, hypoxia, and heart failure. *J. Clin. Invest.* **115,** 500–508
48. Leiro, J. M., Alvarez, E., Arranz, J. A., Cano, E., and Orallo, F. (2004) Antioxidant activity and inhibitory effects of hydralazine on inducible *NOS/COX-2* gene and protein expression in rat peritoneal macrophages. *Int. Immunopharmacol.* **4,** 163–177
49. Janero, D. R., Bryan, N. S., Saijo, F., Dhawan, V., Schwalb, D. J., Warren, M. C., and Feelisch, M. (2004) Differential nitros(yl)ation of blood and tissue constituents during glyceryl trinitrate biotransformation *in vivo*. *Proc. Natl. Acad. Sci. U.S.A.* **101,** 16958–16963
50. Beigi, F., Gonzalez, D. R., Minhas, K. M., Sun, Q. A., Foster, M. W., Khan, S. A., Treuer, A. V., Dulce, R. A., Harrison, R. W., Saraiva, R. M., Premer, C., Schulman, I. H., Stamler, J. S., and Hare, J. M. (2012) Dynamic denitrosylation via *S*-nitrosoglutathione reductase regulates cardiovascular function. *Proc. Natl. Acad. Sci. U.S.A.* **109,** 4314–4319
51. Harrison, C. B., Drummond, G. R., Sobey, C. G., and Selemidis, S. (2010) Evidence that nitric oxide inhibits vascular inflammation and superoxide production via a $p47^{phox}$-dependent mechanism in mice. *Clin. Exp. Pharmacol. Physiol.* **37,** 429–434
52. Shinyashiki, M., Pan, C. J., Lopez, B. E., and Fukuto, J. M. (2004) Inhibition of the yeast metal reductase heme protein fre1 by nitric oxide (NO). A model for inhibition of NADPH oxidase by NO. *Free Radic. Biol. Med.* **37,** 713–723
53. Cote, C. G., Yu, F. S., Zulueta, J. J., Vosatka, R. J., and Hassoun, P. M. (1996) Regulation of intracellular xanthine oxidase by endothelial-derived nitric oxide. *Am. J. Physiol.* **271,** L869-L874
54. Thadani, U., and Whitsett, T. (1988) Relationship of pharmacokinetic and pharmacodynamic properties of the organic nitrates. *Clin. Pharmacokinet.* **15,** 32–43
55. Gogia, H., Mehra, A., Parikh, S., Raman, M., Ajit-Uppal, J., Johnson, J. V., and Elkayam, U. (1995) Prevention of tolerance to hemodynamic effects of nitrates with concomitant use of hydralazine in patients with chronic heart failure. *J. Am. Coll. Cardiol.* **26,** 1575–1580
56. Daiber, A., Mülsch, A., Hink, U., Mollnau, H., Warnholtz, A., Oelze, M., and Münzel, T. (2005) The oxidative stress concept of nitrate tolerance and the antioxidant properties of hydralazine. *Am. J. Cardiol.* **96,** 25i-36i
57. Münzel, T., Daiber, A., and Mülsch, A. (2005) Explaining the phenomenon of nitrate tolerance. *Circ. Res.* **97,** 618–628
58. Bauer, J. A., and Fung, H. L. (1991) Concurrent hydralazine administration prevents nitroglycerin-induced hemodynamic tolerance in experimental heart failure. *Circulation* **84,** 35–39